Chalcogenide Letters Vol. 20, No. 9, September 2023, p. 685 - 695

Enhancing tribological properties of $MoSe_2/SnSe_2/SnSe$@C through 2D nanosheets modification of 3D structures

C. T. Zhu, F. Chen, W. Yan, Y. C. Wei, J. Xu, Y. P. Chen*
School of Physics and Electronic Engineering, Jiangsu University, Zhenjiang, Jiangsu, 212013, P. R. China
Quantum Sensing and Agricultural Intelligence Detection Engineering Center of Jiangsu Province, Zhenjiang, Jiangsu, 212013, P. R. China

This paper has prepared a new type of MoSe2/SnSe2/SnSe@C heterostructure nanocomposites by one-step hydrothermal method and systematically studied by XRD, SEM, and XPS. Furthermore, the tribological behavior of $MoSe_2/SnSe_2/SnSe$ and $MoSe_2/SnSe_2/SnSe$@C heterojunction in pure oil was extensively examined in a ball-on-disk tribometer. The effects of applied load and rotational speed were also investigated. Compared with $MoSe_2/SnSe_2/SnSe$ nanocomposites, $MoSe_2/SnSe_2/SnSe$@C achieved better friction properties. Especially, when the mass ratio of $MoSe_2/SnSe_2/SnSe$@C in the base oil is 1.5 wt%, the friction coefficient reaches the minimum value of 0.1. The results show that the introduction of carbon material can significantly improve the wear reduction and anti-wear properties of the matrix in lubricating oil. Additionally, the construction and excellent tribological properties of $MoSe_2/SnSe_2/SnSe$@C heterojunction would be beneficial for the design of novel nano-additives with 2D/3D structure for enhancing friction reduction and anti-wear, which also would expand their actual applications in the industry and agriculture.

(Received July 5, 2023; Accepted September 18, 2023)

Keywords: $MoSe_2/SnSe_2/SnSe$, Heterojunction, 2D/3D structure, Tribological properties

1. Introduction

As we know, friction is universal in modern industry. Without friction, all mechanical components cannot work. Furthermore, friction and wear are the major causes of the loss of materials and energy[1-5]. Generally, lubricants have been considered the most effective approach to reduce friction and wear and prolong the service life of machines for energy loss. Recently, many inorganic nanoparticles have been widely concerned as promising and potential lubricants due to their excellent friction-reducing and anti-wear performances[6-8]. Therefore, exploring and developing novel inorganic nanoparticles or their composites for enhancing their tribological properties is the biggest challenge at present.

* Corresponding author: chenyuanping2023@163.com
https://doi.org/10.15251/CL.2023.209.685

Nowadays, transition metal selenides (MSe_2, M is the transition metal) have gained considerable attention in the search for novel nano-lubricants to reduce friction and wear because of their lamellar structures and easy interlayer sliding ascribed to the weak van der Waals interactions within their molecular layers[9-11]. In the characteristic layered structure of MSe_2, an M atomic layer sandwiched two Se atomic layers. The intralaminar of the Se–M–Se layer is strong covalent, while the interlayer of the sandwiched structure is weak V a der Waals force, resulting from the decrease in friction coefficient and possessing enhanced reducing-friction and anti-wear properties. More importantly, nano-sized MSe_2 shows more excellent tribological properties compared to commercial MSe_2, which can be applied in harsh working environments, e.g. high pressure and high vacuum[12-16].

Carbon has tremendous potential to be used as an additive to liquid lubricants and/or reinforcements for solid lubricants due to its sp2-hybridized tubular structure, large specific surface area, high strength, and lightweight. Especially, 3D carbon structures have been considered an extreme, promising candidate for the modification of traditional lubricating materials, which can unequivocally enhance the friction reduction and anti-wear properties of matrix or lubricating oil[17-22]. Many recent reports have proved that 3D C/MS_2 composites can effectively improve the tribological properties of base-lubricating materials using as coating film or solid additives of the matrix, and lubricant additives. Zhang et al. have confirmed that CNTs/MoS_2 hybrids consisting of CNTs and MoS_2 NPs, containing liquid lubricants could reduce the COF of pure oil more than that of the pure CNTs and MoS_2. For this reason, integrating a 3D carbon structure has been exemplary and suitable for the modification of layered MS_2 nanomaterials. MSe_2 and MS_2 have the same structure and performance. Therefore, as a result, 3D carbon recombines with MSe_2 would contribute a promising method to design and develop MSe_2-based nano-lubrication for enhancing the tribological behaviors of traditional liquid lubricants[23-29].

Herein, novel MSSC heterojunctions were constructed and synthesized by a one-step hydrothermal approach using C as the precursor. Their frictional and wear behaviors were comparatively investigated by a ball-on-disk tribometer. Furthermore, the morphology and composition of the wear tracks were characterized by SEM, SMP, and EDX technologies, which were conducted to understand their friction and wear mechanisms. Thus the construction and excellent tribological properties of $MoSe_2$/$SnSe_2$/SnSe@C heterojunction would be beneficial for the design of novel nano-additives with 2D/3D structure for enhancing friction reduction and anti-wear, which also would expand their actual applications in the industry and agriculture.

2. Experimental

2.1. Synthesis of ZIF-8

We synthesized ZIF-8 using a simple self-assembly method. Specifically, 0.735 g of zinc nitrate hexahydrate ($Zn(NO_3)_2 \cdot 6H_2O$) and 0.6077 g of dimethylimidazole ($C_4H_6N_2$) were sequentially dissolved in 70 ml of methanol. The mixture was continuously stirred at room temperature for one hour, followed by multiple centrifugation steps using methanol. The resulting white powder was then dried at 80 °C in a vacuum oven. This obtained white powder is referred to as ZIF-8.

2.2. Synthesis of C

The obtained ZIF-8 was placed in a ceramic boat, which was then positioned inside a tubular furnace filled with argon gas. The tubular furnace was heated at a rate of 5 °C per minute until it reached 600 °C and held at that temperature for two hours. After the tubular furnace naturally cooled down to room temperature, a black sample was collected and named C.

2.3. Synthesis of MSSC

0.4 mmol of sodium molybdate dihydrate ($Na_2MoO_4 \cdot 2H_2O$) and 0.1 mmol of sodium stannate trihydrate ($Na_2SnO_3 \cdot 3H_2O$) were sequentially dissolved in 10 ml of deionized water with thorough stirring until complete dissolution, forming solution A. Then, 1.15 mmol of hydrazine hydrate (N_2H_6O) was dissolved in another 10 ml of deionized water and sonicated for 8 minutes, forming solution B. Next, solution B was poured into solution A and stirred for an additional 30 minutes. Subsequently, the previously obtained precursor C was added to the mixed solution of A and B with different masses and stirred for another 30 minutes. Finally, the mixed solution was transferred to a reaction vessel and placed in an oven with a temperature set at 200 °C for 15 hours. After the oven naturally cooled down to room temperature, the mixture was washed several times with deionized water and ethanol. The washed sample was then dried at 60 °C in a vacuum oven. Depending on the amount of added precursor, the final samples were named $MoSe_2/SnSe_2/SnSe$@C(MSSC). The sample without the addition of C precursor was named MSS.

2.4. Characterization

XRD (Bruker-AXS), XPS (Thermo Scientific K-Alpha+ system), Raman Microscope (DXR-Thermo Scientific), SEM (JEOL JXA-840A), and TEM analysis (JEOL JEM-2100) are performed to investigate the phase compositions, chemical states and microstructure of the as-prepared products.

2.5. Tribological Test

The friction reduction and anti-wear of pure base oil containing various nano-additives were investigated by a ball-on-disk tribometer (MS-T3001, China). In our experiments, pure oil was selected as the lubricating oil. During experiments, the rotary velocity of the steel ball was kept at 300 rpm, and the applied load was set to 6 N for 0.5 h at room temperature. Also, different tribological variables including the additive concentration (0.5-2.5 wt %), rotary velocity (100-400 rpm), and applied load (4-10 N) were investigated. More importantly, all friction experiments were investigated three times, respectively. Afterward, the surface roughness and elemental composition of the worn surfaces were quantified by non-contact optical 3D profilers (SMP, NT1100, Veeco WYKO, USA), Atomic Force Microscopy (AFM, MFP-3D, USA), and SEM-EDS analysis (HITACHI S-3400N, Japan).

3. Results and discussion

To investigate the crystal structures of different sample compositions, we performed X-ray diffraction (XRD) tests on the four samples: MSS, and MSSC. As shown in Figure 1, the XRD test of the MSSC nanocomposite material revealed diffraction peaks at 13.7°, 31.4°, 37.8°, 55.9°, and

56.9°, corresponding to the (002), (100), (103), (110), and (008) crystal planes of $MoSe_2$, respectively. All the diffraction peak positions closely matched those of $MoSe_2$ in the standard PDF card (JCPDS NO.29-0914), indicating the synthesis of high-purity $MoSe_2$. However, the overall crystallinity was relatively poor, and an additional diffraction peak at 14.3° was observed, attributed to $SnSe_2$ (JCPDS NO.38-1055). The diffraction peaks at 30.6° and 37.6° were assigned to the (040) and (131) crystal planes of SnSe, respectively. To understand the crystalline variations of samples with different proportions, we obtained XRD images for other compositions, as shown in the following figure. The XRD tests confirm the successful synthesis of $MoSe_2$/$SnSe_2$/SnSe composite materials.

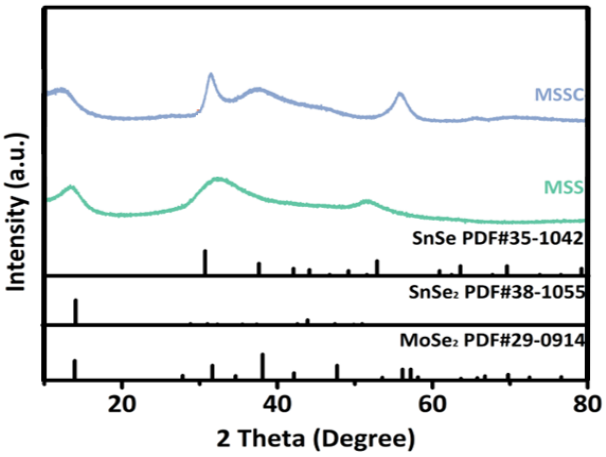

Fig. 1. XRD patterns of MSS, and MSSC.

After determining the crystal structures of the samples, we proceeded to characterize the samples at the microscale using scanning electron microscopy (SEM). As shown in Fig. 2a, the MSS sample exhibits an unordered columnar structure under SEM, with column dimensions on the order of tens of nanometers. However, after incorporating the MOF framework, as shown in Fig. 2b, the MSSC material uniformly grows in situ on the dodecahedral framework derived from ZIF-8. The framework size is approximately 500 nm and some MSS particles that are not attached to the framework aggregate together. Through SEM analysis, we have confirmed that the MSS material is uniformly loaded onto the dodecahedral framework composed of carbon derived from ZIF-8.

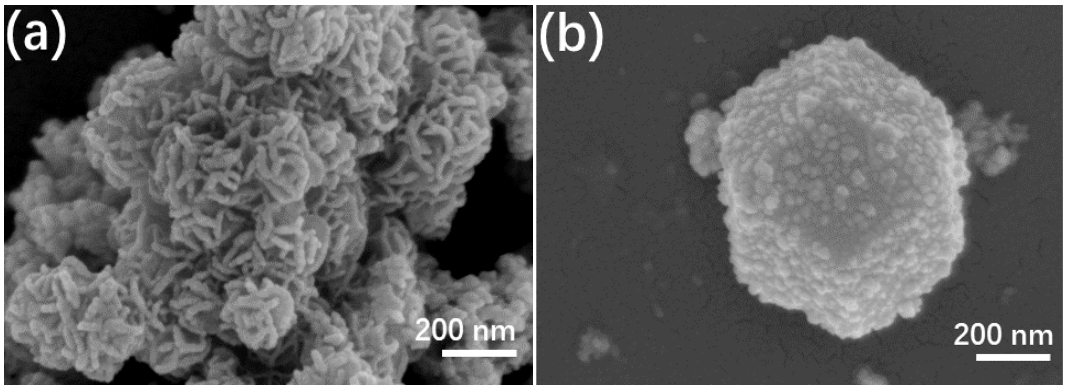

Fig. 2. (a) SEM image of MSS; (b) SEM images of MSSC.

We employed X-ray photoelectron spectroscopy (XPS) analysis to investigate the chemical states and main components of the MSSC-200 sample. The high-resolution XPS spectrum of the C 1s peak could be fitted into three peaks, with binding energies at 288.5, 286.6, and 284.8 eV, corresponding to the C=O bond, C-O bond, and C-C/C=C bond[30-31], respectively (Fig. 3a). Furthermore, the electronic states of Se in the MSSC-200 sample were also studied. As depicted in Fig. 3b, the binding energies at 54.78 and 53.82 eV in the high-resolution Se 2p XPS spectrum can be attributed to the Se $3d_{3/2}$ and Se $3d_{5/2}$ orbitals, respectively[32]. The characteristic peaks at 229.2 eV and 232.2 eV in the Mo 3d high-resolution XPS spectrum are attributed to the Mo $3d_{5/2}$ and Mo $3d_{3/2}$ orbitals of Mo^{4+}, respectively. Additionally, two small peaks observed at 235.6 and 232.9 eV correspond to the Mo $3d_{3/2}$ and Mo $3d_{5/2}$ orbitals of Mo^{6+}, indicating partial oxidation of the $MoSe_2$ sample in the air[32](Fig. 3c). Furthermore, a small peak around 226.2 eV can be attributed to the Se 3s peak. The XPS fine spectrum of Sn (Fig. 3d) reveals that the peaks at binding energies of 494.7 and 486.5 eV are assigned to the $3d_{3/2}$ and $3d_{5/2}$ orbitals of Sn^{4+}, while the peaks at 493.1 and 484.4 eV correspond to the $3d_{3/2}$ and $3d_{5/2}$ orbitals of Sn^{2+}[33]. These analyses further confirm the successful synthesis of the MSSC composite material.

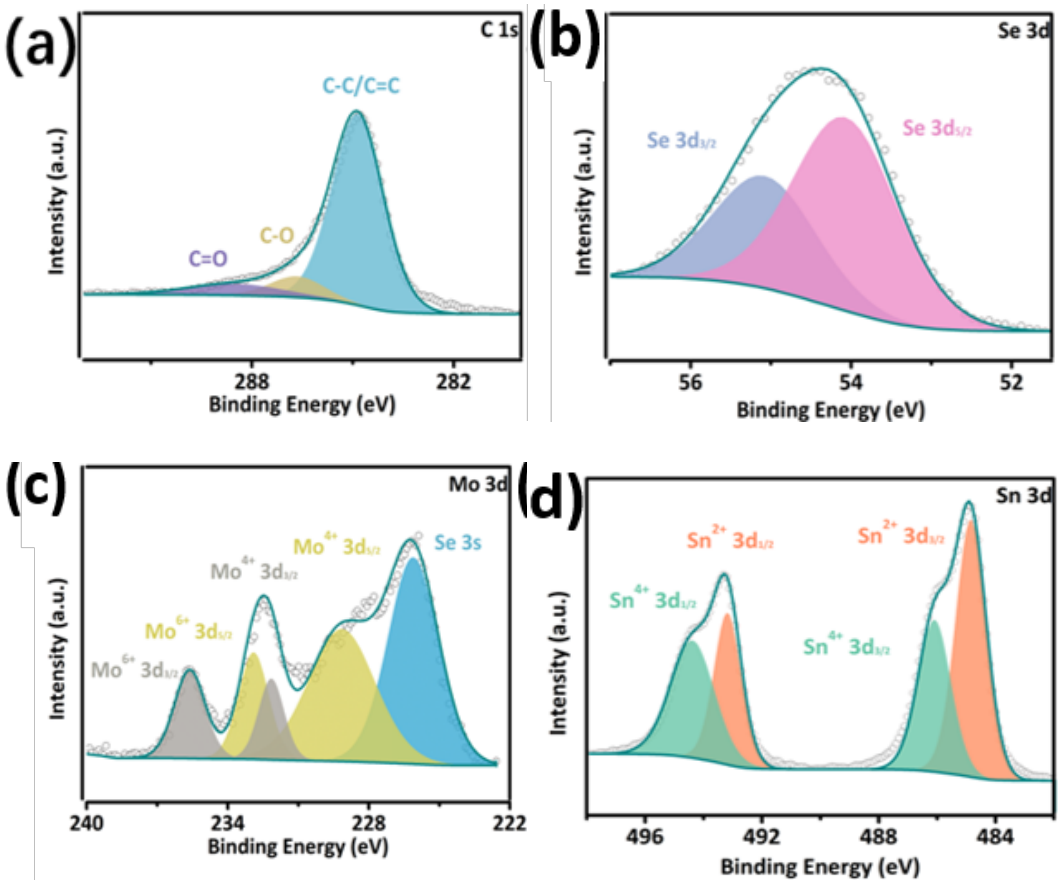

Fig. 3. (a) High-resolution XPS spectra of C 1s;(b) Se 3d; (c) Mo 3d; (d) Sn 3d.

To explore the tribological properties of $MoSe_2/SnSe_2/SnSe$@C nanocomposites, their friction coefficients were tested under the same experimental conditions. As shown in Fig. 4a, the corresponding friction coefficients of MSSC composites in the tribological tests were far lower than those of pure oil, pure C, and $MoSe_2/SnSe_2/SnSe$ composites. It shows that the lubricating

performance of MSSC additive oil is higher than that of pure oil, single phase C, $MoSe_2/SnSe_2/SnSe$ additive oil. Compared Composite monomial, the friction coefficient of MSSC is significantly lower than that of the Composite monomial. Next, different contents of MSSC nanocomposites were added to the base oil to explore the optimal oil-material ratio of MSSC nanocomposites in the base oil, as shown in Fig. 4b. The friction properties of MSSC nanocomposites were tested at different addition levels (0.5 wt%, 1 wt%, 1.5 wt%, 2 wt%, and 2.5 wt%). As can be seen from the friction coefficient in the figure, when the mass ratio of MSSC in the base oil is 1.5 wt%, the corresponding friction coefficient is 0.1. To further analyze the tribological properties of MSSC composites, The tribological behavior of composite samples was tested by applying load (4-10 N) and rotating speed (100-400 rpm), and comparison experiments were carried out with pure oil, C, $MoSe_2/SnSe_2/SnSe$ and MSSC as additives. At a constant speed (200 rpm), the friction curves of pure oil with different additives all show similar trends. First, we tested the friction coefficients of pure oil, C, $MoSe_2/SnSe_2/SnSe$, and MSSC under different loads at the same speed of 300rpm and the optimal oil-material ratio of 1.5 wt%. Under a load of 6 N, the average friction coefficient of MSSC was significantly reduced to 0.1, as shown in Fig. 4c. Similarly, as the speed increases, the average friction coefficient curve shows a trend of first decreasing and then increasing, as shown in Fig. 4d. The lowest average friction coefficient appeared at 300 rpm, which was mainly due to the addition of $MoSe_2/SnSe_2/SnSe$.

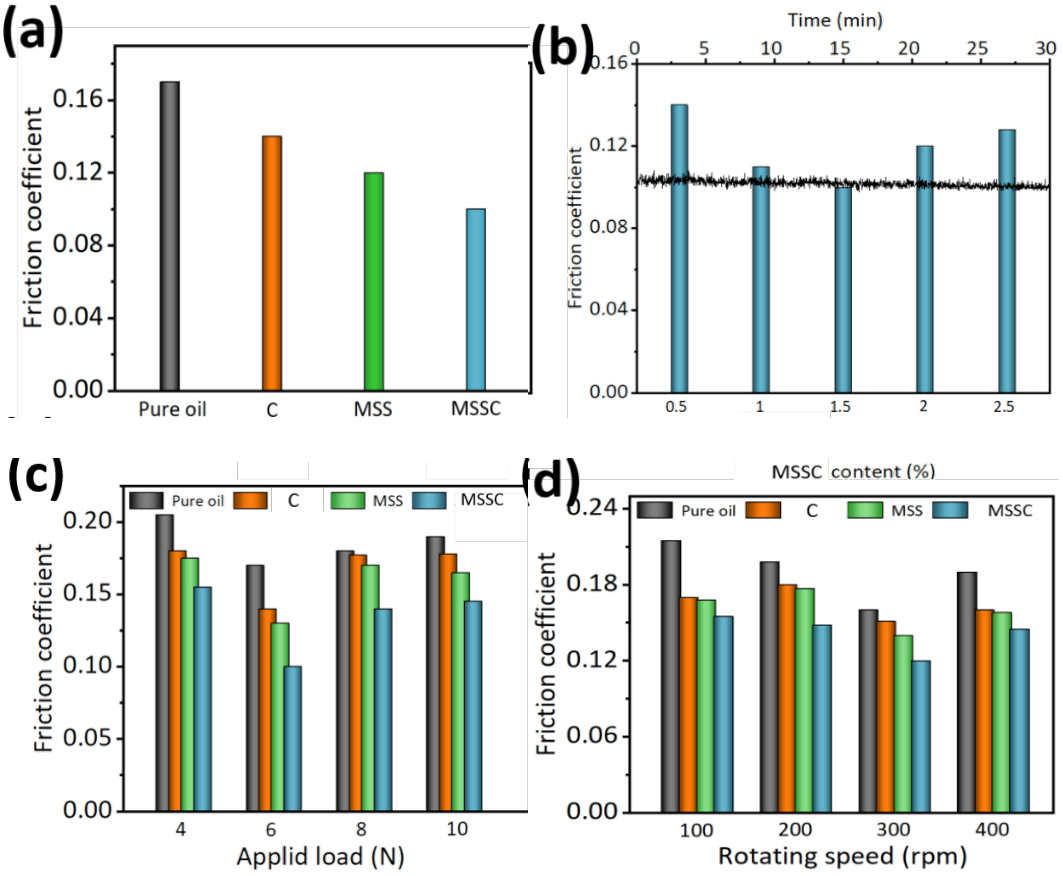

Fig. 4 (a) Friction coefficient of pure oil contained with various oil additives; (b) Friction coefficient of pure oil contained with different MSSC composites additive; Variations of mean friction coefficient of pure oil with different additive (c) increasing load (4-10 N), (d) under diverse speeds (100-400 rpm).

For further study of the wear resistance tribological properties of the MSSC nanocomposites, the topography of the worn scar was investigated using an SEM. Fig. 5 shows the wear scar diagram of the base oil with different additive contents at a speed of 300 rpm and a load of 6 N. Fig. 5a is the wear scar of the steel disc. Fig. 5b is the wear scar diagram of pure base oil, it can be seen that the wear scar is very rough, with a large number of deep furrows appearing and a small amount of sticking occurring, which indicates that the direct contact of the friction pairs results from the damage of the pure base oil film under high load. Fig. 5c and d (the pure oil containing C nanoplates and MSS particles) show that there are only a few furrows and no signs of adhesive wear, indicating that C and MSS particles act as better additives to make the antiwear and antifriction performance of the lubricating oil greatly improved. As shown in Fig. 5d, the surface lubricated with MSSC only presents slender furrows and the friction performance is the best compared with C, and MSS.

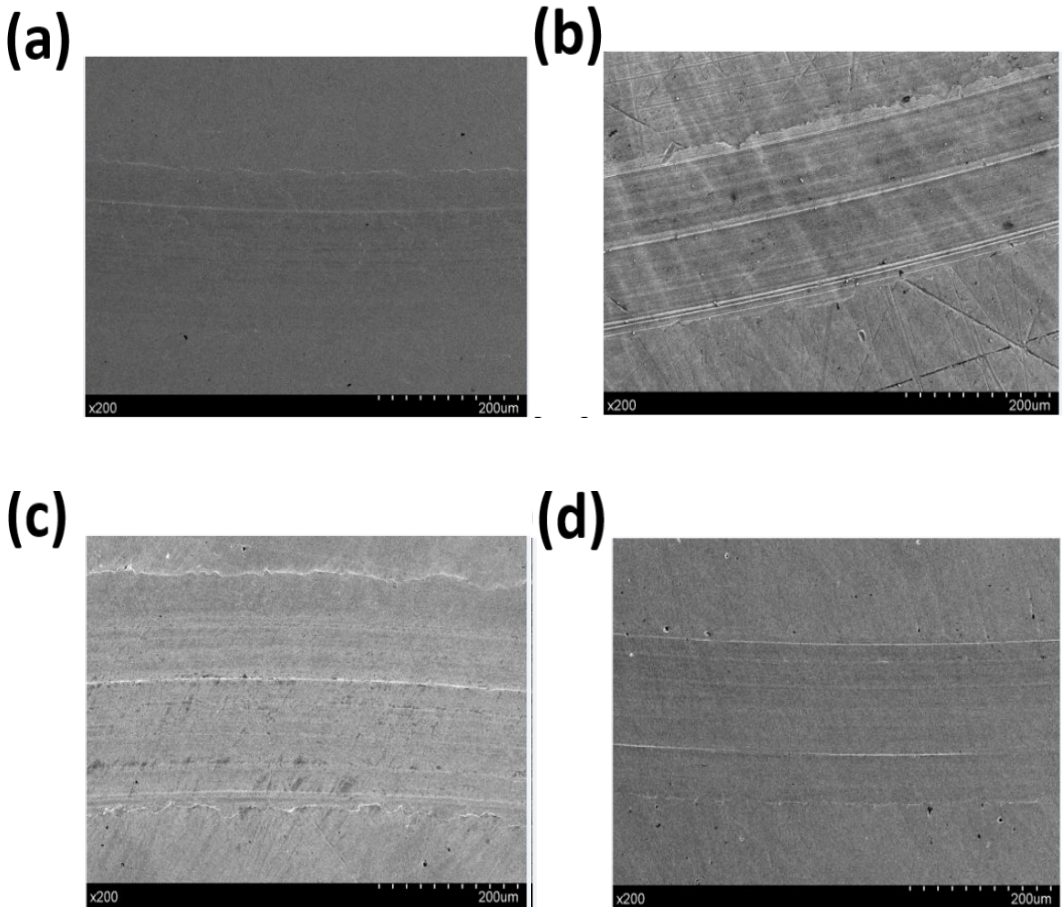

Fig. 5. SEM images of worn surfaces of (a) pure oil, and pure oil contained with (b) C; (c) $MoSe_2$/$SnSe_2$/SnSe, and (d) MSSC composites.

We analyzed the depth and width of the wear marks of the above circular steel disk using a non-contact ultra-depth of field 3D microscope, as shown in Fig. 6. In the Figure, we can see that the depth and width of pure oil wear marks are 4.81 μm and 306.6 μm. The wear depth and width of C composite phases are 2.44 μm and 293.6 μm respectively. The depth and width of wear marks

corresponding to MSS's additive pure oil are 2.324 μm and 279.8 μm, respectively. We then observed the depth and width of the wear trace corresponding to the MSSC additive pure oil. The depth and width of the wear trace were significantly reduced, corresponding to 1.468 μm and 160.1 μm respectively, indicating that the wear reduction effect after the composite is very obvious, and it can also be determined that MSS's nanosheets play a crucial role in the friction test.

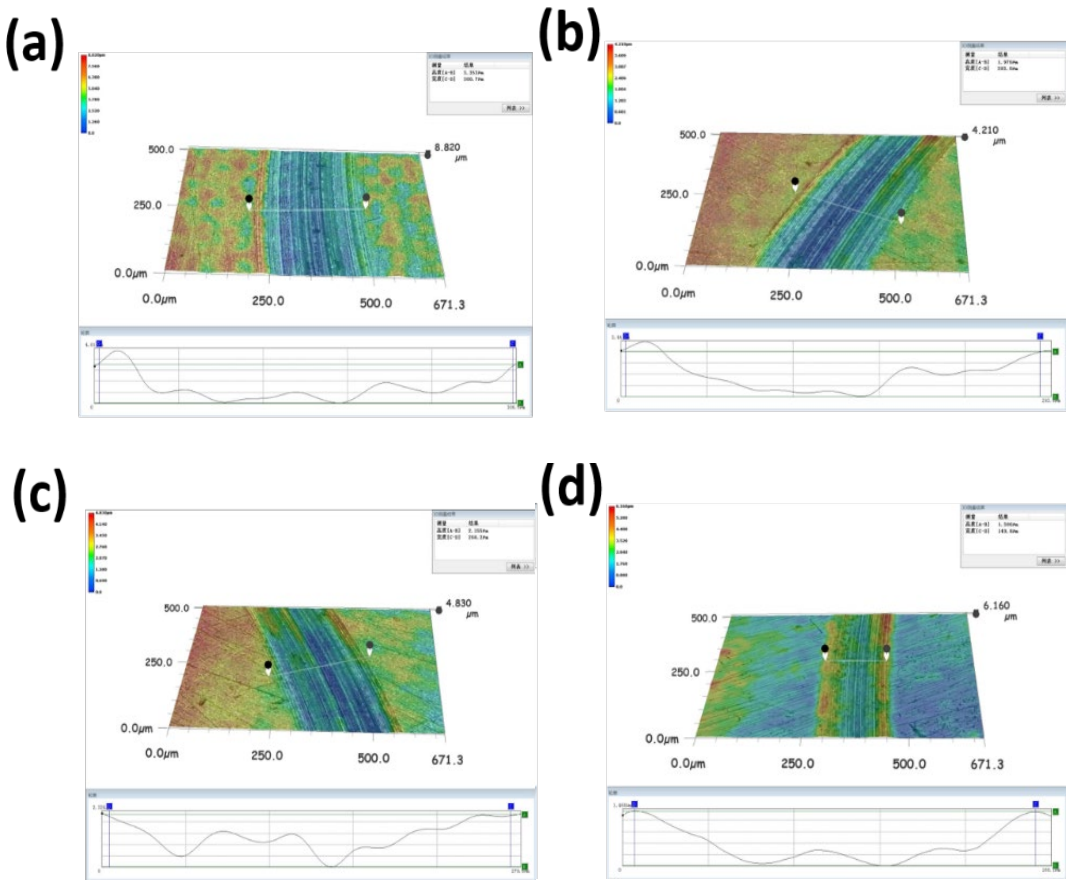

Fig 6. Noncontact three-dimensional images of worn surfaces of (a) pure oil; and pure oil contained with (b) C; (c) $MoSe_2$/$SnSe_2$/SnSe and (d) MSSC composites.

According to the above tribological experimental results and related analysis by many recent reports, an underlying microscopic tribological mechanism was proposed and illustrated in Fig.7. The improvement of friction and wear performance of the MSSC composite is mainly attributed to its unique microstructure and material uniformity. The small and uniform size enables the composite to form a thin layer on the substrate to reduce contact and reduce the generation of wear marks. Moreover, MSSC can be adsorbed and deposited on the rubbing interfaces, which hindered the direct contact between the interfaces of the steel disc and ball, resulting in excellent antiwear ability. The conclusion on the wear mechanism of the composite by the debris topography analysis is coincident with that of the SEM analysis on the worn surface.

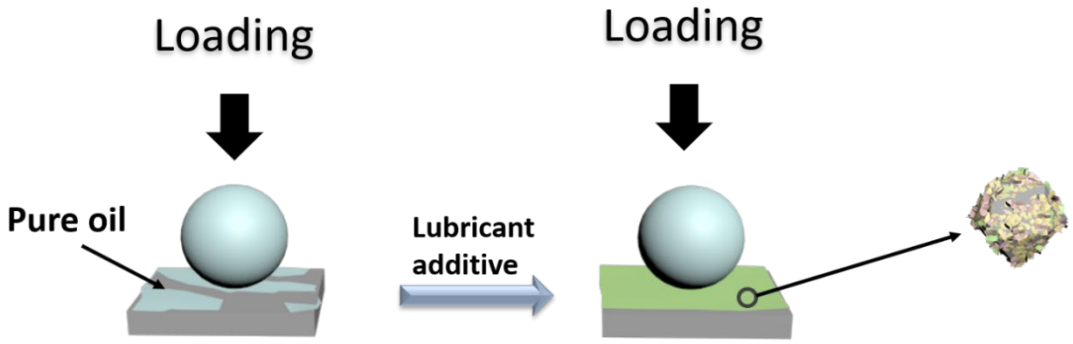

Fig. 7. The tribological mechanism of MSSC additive in liquid paraffin.

4. Conclusions

In this paper, a simple one-step hydrothermal method was used to successfully synthesize metallic $MoSe_2/SnSe_2/SnSe$@C and use it as a new lubricant additive for pure oil. The characterization results show that the nanocomposite is more uniformly dispersed. In addition, the tribological behavior of nanocomposite in pure oil has been extensively studied using a ball-disk tribometer. The 2D/3D $MoSe_2/SnSe_2/SnSe$@C heterojunction is constructed by combining the advantages of MSe_2 and carbon materials in improving the anti-friction and anti-wear properties of the substrate or lubricant. The results show that the introduction of nanocomposite significantly reduces friction and wear in water-based drilling fluids. Among them, the 1.5 wt% nanocomposite to pure oil ratio has the lowest friction coefficient. The results show that nanocomposite exhibits excellent anti-friction and wear properties in pure oil, which is conducive to the design of new nano-additives to improve friction and wear properties.

Acknowledgments

This research was supported by the Natural Science Foundation of the Chinese Academy of Sciences, the National Natural Science Foundation of China (12074150, 12174157, 12174158, 11874314), the Key Research and Development Project of Chang Zhou (Grant no. CJ20220039) , and the Research Start-up Project of Jiangsu University (No.20JDG44).

References

[1] X Zhang, Z Cai, X Zhang, J Wang, Q Wang, Wear, 2018, 408-409: 1-10.

[2] C Y Min, Z B He, H J Song, H Y Liang, D D Liu, C K Dong, W Jia, Tribology International, 2019, 140: 9-16; https://doi.org/10.1016/j.triboint.2019.105867

[3] H Shi, S Du, C Sun, C Song, Z Yang, Y Zhang, Materials, 2019, 12 (22): 3680; https://doi.org/10.3390/ma12010045

[4] R Zhang, D Qiao, X Liu, Industrial & Engineering Chemistry Research, 2018, 57 (29): 10379-10390; https://doi.org/10.1021/acs.iecr.8b01694

[5] J Xu, H Tang, G Tang, Chalcogenide Letters, 2014, 11 (6): 265-267.

[6] H Mishina, Journal of the Japan Society of Tribologists, 2012, 57 (5): 303-308.

[7] S Lin, H Wang, X Zhang, D Wang, D Zu, J Song, Z Liu, Y Huang, K Huang, N Tao, Z Li, X Bai, B Li, M Lei, Z Yu, H Wu, Nano Energy, 2019, 62: 111-116; https://doi.org/10.1016/j.nanoen.2019.04.071

[8] Y Wang, L Cui, G Cheng, N Yuan, J Ding, N S Pesika, Tribology Letters, 2018, 66 (4): 148; https://doi.org/10.1007/s11249-018-1102-2

[9] J. Xu, H.Tang, Q. Shi, CS.Li, Chalcogenide Letters, 2015, 12(1), 1-10

[10] Y Li, H Lu, Q Liu, L Qin, G Dong, Tribology International, 2019, 137: 22-29; https://doi.org/10.1016/j.triboint.2019.04.029

[11]Shi,Q, Xu.J; Dang,LF; Chen,J; Tang,GG; Li,CS, Journal of Nano Research ,2017,45,34-41; https://doi.org/10.4028/www.scientific.net/JNanoR.45.34

[12] D S Li, H C Wang, H Tang, X F Yang, Q Q Liu, ACS Sustainable Chemistry & Engineering, 2019, 7 (9): 8466-8474; https://doi.org/10.1021/acssuschemeng.9b00252

[13] B Wetzel, F Haupert, M Q Zhang, Composites Science and Technology, 2003, 63 (14): 2055-2067; https://doi.org/10.1016/S0266-3538(03)00115-5

[14] L Zhao, H Yang, C Liu, S Xue, Z Deng, J Li, X Zeng, Tribology Letters, 2019, 67 (3): 85; https://doi.org/10.1007/s11249-019-1199-y

[15] Y. Jiang, K. Shi, H. Tang, Y. Wang, Surf. Coat. Technol. 374 (2019) 1258-1266; https://doi.org/10.1016/j.surfcoat.2019.07.051

[16] G Tang, F Zhang, J Xu, Micro & Nano Letters, 2019, 14 (12): 1394-1398; https://doi.org/10.1049/mnl.2018.5420

[17] W X Chen, J P Tu, L Y Wang, et al., Carbon, 2003, 41 (2): 215-222; https://doi.org/10.1016/S0008-6223(02)00265-8

[18] R H Baughman, A A Zakhidov, W A de Heer, Science, 2002, 297 (5582): 787-792; https://doi.org/10.1126/science.1060928

[19] S Kanagaraj, F R Varanda, T V Zhil'tsova, et al., Composites Science and Technology, 2007, 67 (15-16): 3071-3077; https://doi.org/10.1016/j.compscitech.2007.04.024

[20] D Tasis, N Tagmatarchis, A Bianco, M Prato, Chemical Reviews, 2006, 106 (3): 1105-1136; https://doi.org/10.1021/cr050569o

[21] D Qian, E C Dickey, R Andrews, T Rantell, Applied Physics Letters, 2000, 76 (20): 2868-2870; https://doi.org/10.1063/1.126500

[22] J Xu, L Dong, K Zhang, C Li, Journal of Wuhan University of Technology, 2017, 32 (1): 1-5; https://doi.org/10.1007/s11595-017-1553-6

[23] L Wei, Y Zhang, C Xu, F Qi, S Meng, Journal of Central South University, 2012, 19 (10): 2878-2883; https://doi.org/10.1007/s11771-012-0969-6

[24] B Chen, Q Ding, D Ni, et al., Journal of Advanced Ceramics, 2021, 10 (3): 657-667; https://doi.org/10.1007/s40145-020-0414-5

[25] J Liang, Z Liang, Z Zhang, W Liu, Journal of Materials Science, 2019, 54 (15): 10665-10678; https://doi.org/10.1007/s10853-019-03723-1

[26] J Liang, Z Liang, Z Zhang, W Liu, Tribology International, 2020, 150: 106403.

[27] Y Wang, J Wang, L Wang, W Liu, Applied Surface Science, 2018, 427 (A): 1019-1026.

[28] Y Wang, J Wang, L Wang, W Liu, Ceramics International, 2019, 45 (17): 22376-22383.

[29] Y Zhang, W Liu, X Wang, Y Liu, Materials Letters, 2014, 131: 248-251; https://doi.org/10.1016/j.matlet.2014.06.006

[30] W Yan, Y Xu, S Hao, Z He, L Wang, Q Wei, J Xu, H Tang, Inorganic Chemistry, 2022, 61 (11): 4725-4734; https://doi.org/10.1021/acs.inorgchem.2c00045

[31] YY Xu, W Yan, X Sun, G Tang, Y Chen, J Xu, Ceramics International, 2022, 6: 7687-7694; https://doi.org/10.1016/j.ceramint.2021.11.316

[32] A Kozak, M Precner, P Hutár, M Bodík, K Vegso, Y Halahovets, M Hulman, P Siffalovic, M Ťapajna, Applied Surface Science, 2021, 571: 150807; https://doi.org/10.1016/j.apsusc.2021.150807

[33] C Lua, Y Zhang, L Zhang, Q Yina, Applied Surface Science, 2021, 560: 150174; https://doi.org/10.1016/j.apsusc.2019.04.104